

|                             |   |
|-----------------------------|---|
| Title                       | Solid-state characterization of novel active pharmaceutical ingredients: Cocrystal of a salbutamol hemiadipate salt with adipic acid (2:1:1) and salbutamol hemisuccinate salt.   |
| Authors                     | Paluch, Krzysztof J.;Tajber, Lidia;Elcoate, Curtis J.;Corrigan, Owen I.;Lawrence, Simon E.;Healy, Anne Marie  |
| Publication date            | 2011-04   |
| Original Citation           | Paluch,Krzysztof J.,Tajber,Lidia,Elcoate,Curtis J.,Corrigan,Owen I.,Lawrence,Simon E.,Healy,Anne Marie. (2011) 'Solid-state characterization of novel active pharmaceutical ingredients: Cocrystal of a salbutamol hemiadipate salt with adipic acid (2:1:1) and salbutamol hemisuccinate salt'. Journal of Pharmaceutical Sciences, 100 (8):3268-3283.   |
| Type of publication         | Article (peer-reviewed)   |
| Link to publisher's version | 10.1002/jps.22569   |
| Rights                      | © 2011 Wiley-Liss, Inc. and the American Pharmacists Association. This is the pre-peer reviewed version of the following article: PALUCH, K. J., TAJBER, L., ELCOATE, C. J., CORRIGAN, O. I., LAWRENCE, S. E. & HEALY, A. M. 2011. Solid-state characterization of novel active pharmaceutical ingredients: Cocrystal of a salbutamol hemiadipate salt with adipic acid (2:1:1) and salbutamol hemisuccinate salt. Journal of Pharmaceutical Sciences, 100, 3268-3283., which has been published in final form at <a href="http://dx.doi.org/10.1002/jps.22569">http://dx.doi.org/10.1002/jps.22569</a> . |
| Download date               | 2025-01-13 23:09:35   |
| Item downloaded from        | <a href="https://hdl.handle.net/10468/1419">https://hdl.handle.net/10468/1419</a>   |



**University College Cork, Ireland**  
Coláiste na hOllscoile Corcaigh

# Solid state characterisation of novel active pharmaceutical ingredients: co-crystal of a salbutamol hemiadipate salt with adipic acid (2:1:1) and salbutamol hemisuccinate salt

Krzysztof J. Paluch <sup>a</sup>, Lidia Tajber <sup>a</sup>, Curtis J. Elcoate <sup>b</sup>, Owen I. Corrigan <sup>a</sup>,  
Simon E. Lawrence <sup>b</sup>, Anne Marie Healy <sup>a\*</sup>

*a) School of Pharmacy and Pharmaceutical Sciences Trinity College Dublin, College Green, Dublin 2, Ireland,*

*b) Department of Chemistry, Analytical and Biological Chemistry Research Facility, University College Cork, College Road, Cork, Ireland.*

\* To whom correspondence should be sent. Ph.: 00 353 1896 1444, e-mail: [healyam@tcd.ie](mailto:healyam@tcd.ie)

## Abstract

The production of salt or co-crystalline forms is a common approach to altering the physicochemical properties of pharmaceutical compounds. The goal of this work was to evaluate the impact of anion choice (succinate, adipate and sulfate) on the physicochemical characteristics of salbutamol forms. Novel crystals of salbutamol were produced by solvent evaporation: a co-crystal of salbutamol hemiadipate with adipic acid (SA), salbutamol hemi-succinate tetramethanolate (SSU.MeOH) and its desolvated form (SSU). The crystalline materials obtained were characterized using: thermal, X-ray, NMR, FTIR, DVS and elemental analyses. The crystal forms of SA and SSU.MeOH were determined to be triclinic,  $P\bar{1}$ , and monoclinic,  $P2_1/n$ , respectively. DVS analysis confirmed that SSU and SA do not undergo hydration under increased %RH. Thermal and elemental analyses confirmed the stoichiometry of the salt forms. The aqueous solubilities of SA and SSU were measured to be  $82 \pm 2$  mg/ml (pH  $4.5 \pm 0.1$ ) and  $334 \pm 13$  mg/ml (pH  $6.6 \pm 0.1$ ), respectively. Measured values corresponded well with calculated pH solubility profiles. The intrinsic dissolution rate of co-crystallized SA was approximately four times lower than SSU, suggesting its use as an alternative to more rapidly dissolving salbutamol sulfate.

**Keywords:** co-crystals, crystal structure, desolvation, dissolution rate, solubility, solvate, thermal analysis, water sorption, X-ray powder diffraction.

## Introduction

Salbutamol is a  $\beta$ 2-mimetic used as a bronchodilator which is presented as the ( $\pm$ ) racemic mixture in pharmaceutical inhalers (propellant-based and dry powder), nebules, injections, syrups and tablets, including controlled-release forms<sup>1</sup>. The hemisulfate salt (commonly referred to as salbutamol sulfate) is the most common form of salbutamol used in pharmaceutical products however the (*R*) salbutamol hydrochloride form is also available on the market as an inhalation solution (Xopenex<sup>TM</sup>, manufactured by Sepracor Inc.). Although some other salbutamol salts have been reported in the literature, e.g. ethanolated salbutamol adipate and salbutamol stearate<sup>2</sup>, to date only two crystal structures are reported in the Cambridge Structural Database: salbutamol base (SB)<sup>3</sup> and salbutamol sulfate (SS)<sup>4</sup>. The information about the solid state nature of other forms of salbutamol is sparse.

From a pharmaceutical point of view, different solid-state characteristics of salt forms can result in different *in vitro* solubility and dissolution properties, which in turn can result in an alteration of the *in vivo* activity of the active pharmaceutical ingredient (API). In particular, for pulmonary delivery, possibilities for modification of the dissolution profile of the API from a formulation point of view are limited, due to restrictions in terms of the excipients that are regarded as safe for pulmonary use, and may result in additional costs and regulatory obstacles associated with the development of a new drug product. This may be avoided by the direct production of alternative crystalline forms of the API with the desired solubility and dissolution profiles. The marketed solid dosage forms contain only SS, which is freely soluble in water<sup>5</sup>. The advantage of prolonged release tablets containing SS was reported in clinical studies<sup>6</sup>. New prolonged release oral dosage forms containing SS include hard capsules VentMax<sup>TM</sup> and tablet forms: Volmax CR<sup>TM</sup>, Vospire ER<sup>TM</sup> <sup>7</sup>. Both, prolonged release capsules and tablets containing SS have monographs in the British Pharmacopeia<sup>8</sup>. A transdermal delivery patch of SS was also developed <sup>9</sup>.

In this study we investigated the impact of replacing the sulfate anion in the SS salt structure by an organic dicarboxylic acid, either the four-carbon chain, succinic (butanedioic) acid or the six-carbon

chain, adipic (hexanedioic) acid, on the physicochemical characteristics of the API. These two organic acids were chosen in order to investigate the impact of small changes in the chemical structure of the co-former on the physicochemical properties of the resulting salbutamol forms. A reasonable correlation between the melting points of organic co-formers and melting points of the resulting salts was previously reported for diclofenac<sup>10</sup>. The authors also observed a trend between the salt melting point and the logarithm of the solubility. The reported melting points of adipic and succinic acids are ~151-154 °C and ~185-187 °C, respectively<sup>11</sup>, hence it may be hypothesized that the succinate would have a lower solubility than that of the adipate. On the other hand, increasing the hydrophilicity of the counterion as a means of increasing the water solubility of the resultant salt has been proposed and investigated for a series of erythromycin<sup>12</sup>. The calculated logPs of adipic and succinic acid are 0.356 and -0.655 respectively<sup>13</sup>, indicating that a salt of adipic acid may be less soluble than that of succinic acid. The study performed by Lee et al.<sup>14</sup> successfully investigated the possibility of forming ionic (salts) or neutral (co-crystals) complexes of a heterocyclic base (an ErbB2 inhibitor for the treatment of cancer) with dicarboxylic acids comprising succinate, malonate and maleate co-formers. The acids (adipic and succinic) used in the current study have similar pKa values. The pKa1 and pKa2 for succinic acid are 4.21 and 5.64<sup>11</sup> and for adipic acid these are 4.44 and 5.44<sup>11</sup>. As pKas of salbutamol are 9.1 and 10.4<sup>15</sup>, it was expected that the new forms of the API would be novel 1:1 salts of salbutamol.

Both acids are classified by the U.S. Food and Drug Administration as Generally Recognised As Safe (GRAS)<sup>16,17</sup> and listed in the European Pharmacopeia<sup>5</sup>. Adipic acid is currently used to produce salts of piperazine (Entacyl<sup>TM</sup>) and spiramycine (Rovamycine<sup>TM</sup> injectable form)<sup>11</sup>. Succinic acid is used to form salts of e.g. benfurodil, bamethan, chloramphenicol, cibenzoline, deanol, doxylamine, ergotamine, loxepine, metoprolol, oxaflumazine, sumatriptan and iron (FeII)<sup>11</sup>.

## Materials

Salbutamol base was obtained from CHEMOS GmbH Germany. Adipic acid was obtained from Sigma-Aldrich (Germany) and succinic acid from Sigma-Aldrich Chemical Company (USA) both (99%+ grade). HPLC grade methanol was obtained from Fischer Scientific UK. Deionized water was obtained from a Purite Prestige Analyst HP water purification system. Potassium bromide (KBr, FTIR grade) was obtained from Sigma-Aldrich (Ireland). Deuterated dimethyl sulphoxide (DMSO-d<sub>6</sub>) was obtained from Apollo Scientific Limited (UK) and paraffin wax from BDH Laboratory Supplies Poole, England. All other chemicals were of analytical grade and used without further purification.

## Methods

### Crystallization studies

Attempts were made to crystallize salbutamol with adipic acid and succinic acid by solvent evaporation from ethanol, methanol and water. The tested molar ratios of salbutamol to the acid were: 1:2, 1:1 and 2:1 for each solvent. It was observed that successful crystallization was achieved only for salbutamol mixed with adipic acid in the 1:1 molar ratio using methanol or water as the solvent and for salbutamol and succinic acid mixed in the 2:1 molar ratio using methanol (details of the procedure are described below). Other combinations resulted either in crystallization of one or two of the components separately or in the production of a glassy/amorphous material.

The crystals subsequently used for single crystal X-ray and other analyses were prepared from saturated solutions, which were obtained by introducing an excess of raw material into the appropriate solvent at ambient conditions and shaking for an hour on a WhirliMixer<sup>®</sup> (Fisons Scientific Equipment). 10 mL of the suspension obtained was filtered through a 0.22 µm membrane filter into a glass vial which was kept in a glove box (Clean Sphere CA 100, Safetech Limited) under constant nitrogen flow at room temperature (20-23 °C). The moisture content in this controlled environment was less than 1% relative humidity.

Dry nitrogen flow and temperature control were provided to maintain reproducible conditions of solvent evaporation. Crystallization of SA from methanol resulted each time in a very rapid nucleation of the crystals. Modification of the environmental conditions, including slowing down the evaporation rate of methanol and decreasing the temperature, did not retard the crystal growth. Very small crystals with crystal defects (inclusions) were not of sufficiently good quality to be analyzed by single crystal X-ray analysis. A change of the solvent to water resulted in slow crystal growth and good quality crystals of SA, with a PXRD pattern consistent with that obtained for crystals produced from methanol, hence the SA crystals obtained from water were later used for single crystal X-ray analysis.

### **Preparation of salbutamol adipate and succinate**

A stoichiometric mixture of salbutamol and adipic acid in a 1:1 molar ratio was dissolved in methanol at 0.05 g/mL concentration of solid at 25 °C. Methanol was evaporated under forced air flow at an evaporation rate 0.4 g/min (monitored using a balance every 5 min), whilst stirring. The white precipitate was filtered close to the end of methanol evaporation. The precipitate was dried for an hour under constant air flow at 25 °C. The dry powder was subjected to elemental analysis and was determined to be salbutamol mono adipate (SA). It was obtained with a 95% yield.

A stoichiometric mixture of salbutamol and succinic acid in a 2:1 molar ratio was dissolved in methanol at 0.05 g/mL concentration of solid at 25 °C. Methanol was evaporated under forced air flow at an evaporation rate of 0.4 g/min (monitored using a balance every 5 min), whilst stirring. After nucleation of the salt, the temperature was dropped to 20 °C and the evaporation rate of methanol was kept constant (0.4 g/min) until the concentration of solid in methanol reached 0.1 g/mL. The white precipitate was filtered and dried at 25 °C. Elemental analysis of the white crystalline powder determined it to be salbutamol hemi-succinate tetramethanolate (SSU.MeOH). It was obtained with a 80% yield. Further drying of the precipitate under constant air flow at 25 °C for 24 hr resulted in formation of the desolvated salbutamol hemi-succinate (SSU).

### **Single crystal X-ray diffraction**

X-ray diffraction measurements were made on a Bruker APEX II DUO diffractometer using graphite monochromatized MoK $\alpha$  radiation ( $\lambda = 0.7107 \text{ \AA}$ ) and an Oxford Cryosystems COBRA fitted with a N<sub>2</sub> generator. All calculations were made using the APEX2 software (APEX2 v2009.3-0, Bruker AXS, 2009; Sheldrick, 2008)<sup>18</sup> and the diagrams prepared using Mercury<sup>19</sup>.

CCDC 801059 (SA) and 801060 (SSU.MeOH) contains the supplementary crystallographic data for this paper. These data can be obtained free of charge from The Cambridge Crystallographic Data Centre via [www.ccdc.cam.ac.uk/data\\_request/cif](http://www.ccdc.cam.ac.uk/data_request/cif)

### **Powder X-ray diffraction (PXRD)**

Powder XRD analysis was conducted using a Rigaku Miniflex II Desktop X-ray diffractometer fitted with an Ilaskris cooling unit operating at 30 kV and 15 mA. Ni-filtered Cu-K $\alpha$  radiation ( $\lambda = 1.5408 \text{ \AA}$ ) was used. Room temperature measurements were recorded for the range 5-40° 2 $\theta$  at a step size of 0.05 °/s<sup>20</sup>.

### **Differential scanning calorimetry (DSC)**

DSC experiments were performed using a Mettler Toledo DSC 821<sup>°</sup> with a refrigerated cooling system, LabPlant RP-100. Nitrogen was used as the purge gas. Aluminium sample holders were sealed with a lid and pierced to provide three vent holes. Sample volume was sufficient to provide proper contact between the powder and the bottom of the pan, and sample weight was  $\geq 5$  mg. DSC measurements were carried out at a heating/cooling rate of 10 °C/min<sup>21</sup>. The DSC system was controlled by Mettler Toledo STAR<sup>°</sup> software (version 6.10) working on a Windows NT operating system. The unit was calibrated with indium and zinc standards.



### **Thermogravimetric analysis (TGA)**

TGA was performed using a Mettler TG 50 module linked to a Mettler MT5 balance. Samples were placed into open aluminium pans (5-12 mg). A heating rate of 10 °C/min was implemented in all measurements<sup>21</sup>. Analysis was carried out in the furnace under nitrogen purge and monitored by Mettler Toledo STAR<sup>e</sup> software (version 6.10) with a Windows NT operating system.

### **Solid state Fourier transform infrared spectroscopy (FTIR)**

Infrared spectra were recorded on a Nicolet Magna IR 560 E.S.P. spectrophotometer equipped with MCT/A detector, working under Omnic software version 4.1. A spectral range of 650-4000 cm<sup>-1</sup>, resolution 2 cm<sup>-1</sup> and accumulation of 64 scans were used in order to obtain good quality spectra. A KBr disk method was used with a 0.5-1% sample loading. KBr disks were prepared by direct compression under 8 bar pressure for 1 min<sup>22</sup>. The sample preparation did not affect the spectra, as confirmed with an attenuated total reflectance (ATR) spectrometer (data not shown). The Omnic 4.1<sup>TM</sup> - FTIR spectra analysis with baseline auto correction software was used to analyze the data.

### **Nuclear magnetic resonance (<sup>1</sup>HNMR, <sup>13</sup>CNMR)**

A Bruker Avance 400 NMR with 4-nucleus (<sup>1</sup>H, <sup>13</sup>C, <sup>31</sup>P and <sup>19</sup>F) probe was used for NMR studies. Deuterated DMSO-d<sub>6</sub> was used to prepare the samples. Sample concentration was in the range 20-40 mg/mL. Spectrometer frequency was 400 MHz with an acquisition time of 2 s. The number of scans was appropriate to gain good quality spectra. Standard Pulse Sequence supplied by Bruker was used for <sup>1</sup>H, DEPT-90, DEPT-135, <sup>13</sup>C and 2-dimensional CH-COSY experiments. The TopSpin 2.1<sup>TM</sup> software was used to evaluate <sup>1</sup>HNMR and <sup>13</sup>CNMR results.

## **Elemental analysis**

Elemental analysis was carried out using an Exeter Analytical CE440 CHN analyzer. The molar amount of carbon as carbon dioxide, nitrogen, as nitrogen oxide and hydrogen as water, was determined by oxidation of the sample (around 10 mg) and thermal conductivity analysis of the gases obtained<sup>23</sup>.

## **Dynamic vapor sorption (DVS)**

Vapor sorption experiments were performed on a DVS Advantage-1 automated gravimetric vapor sorption analyzer (Surface Measurement Systems Ltd., London, UK). The temperature was maintained constant at  $25.0 \pm 0.1$  °C. A mass of around 10 mg of powder was loaded into a sample net basket and placed in the system. The samples were equilibrated at 0% of relative humidity (RH) until the dry, reference mass was recorded. The samples were exposed to the following % of RH profile: 0 to 90% in 10% steps and the same for desorption. At each stage, the sample mass was equilibrated ( $dm/dt \leq 0.002$  mg/min for at least 10 min) before the change of relative humidity. An isotherm was calculated from the complete sorption and desorption profile. Amount of water was expressed as a percentage of the reference mass.

## **Specific surface area analysis ( $T_{BET}$ ) by Brunauer, Emmett, Teller (BET) isotherm**

Samples were dried prior to analysis under nitrogen flow at 50°C for 12 hours using a Gemini SmartPrep (USA) drying station. To determine the bulk specific surface area a Micromeritics Gemini VI (USA) surface area analyzer was used. Compressed nitrogen was used as an adsorptive gas. Each measurement consisted of six steps, determining the amount of gas adsorbed at 6 relative pressure points in the range of 0.05 to 0.3 of relative pressure  $P/P_0$  with equilibration time of 10s. Free space was determined separately for each sample using helium gas. Saturation pressure  $P_0$  was determined prior to the measurement of each sample.

## **Particle size**

Measurements of particle size and particle size distributions were obtained using a laser diffraction particle sizer Mastersizer 2000 (Malvern Instruments, UK). Particles were dispersed using a Scirocco dry feeder instrument with 2 bar pressure. An obscuration rate of 0.5-6% was obtained under a vibration feed rate of 50%.

## **Solubility studies**

Powdered SA, SSU and SB were added in excess (approximately three times the expected saturated concentration of salbutamol) directly to 2 ml of water in an Eppendorf vial at 37 °C<sup>24</sup>. Additionally, the SA powder was suspended in a NaOH solution to investigate its solubility at a pH value other than that measured for the sample in pure water. The Eppendorfs were placed horizontally in a water bath and shaken at 100 cpm. Suspensions were filtered through a 0.22 µm membrane filter. The content of salbutamol in the saturated solutions was assayed by UV spectrophotometry at 276 nm (Shimadzu UV 1700 Pharmaspec). SB, SA and SSU aliquots were diluted with water to obtain the appropriate concentration range. Samples were withdrawn and analyzed after 10, 11 and 12 hours and as equilibrium appeared to be reached after 10 hours, the values were averaged over these three time points.

The content of adipic and succinic acids in SA and SSU aliquots was determined with a high pressure liquid chromatography (HPLC). The HPLC system used was a Shimadzu HPLC Class VP series with a LC-10AT VP pump, autosampler SIL-10AD VP and SCL-10AVP system controller. The mobile phase was filtered through a 0.45 µm membrane filter (Gelman Supor-450, USA) before use. The HPLC method used for the analysis of the dicarboxylic acids was modified from Thoma and Ziegler<sup>25</sup> and Kordis-Krapez et al.<sup>26</sup>. The analytical column used was a LiChrosorb RP-10 column (250 mm length, internal diameter 4 mm, particle size 10 µm). UV detection was carried out at a wavelength of 210 nm and the injection volume was 20 µL.

Separation of adipic acid was carried out isocratically at ambient temperatures with a flow rate of 1 ml/min. The mobile phase consisted of methanol:phosphoric acid solution (pH 2.1) 20:80 (v/v).

Separation of succinic acid was carried out using a gradient method with a flow rate of 1 ml/min. The mobile phase consisted of two eluents: (A) phosphoric acid solution (pH 2.1) and (B) methanol:phosphoric acid solution (pH 2.1) 20:80 (v/v). The following gradient was used: a linear gradient from 0 to 50% B over 7 min, then a linear gradient from 50 to 100% B over 1 min and this composition was maintained for 7 min. Then again a linear gradient from 100 to 0% B over 10 min was applied and the final mobile phase composition was continued for a further 5 min. Under these conditions the retention times of adipic acid and succinic were: 4.3 and 6.5 min, respectively.

### **Intrinsic dissolution studies**

Discs of SS, SSU and SA were prepared by compressing 300 mg of the given material in an IR hydraulic press (PerkinElmer, UK). The 13 mm diameter discs had a  $1.33 \text{ cm}^2$  top surface area. The bottom and side surfaces of the discs were coated with paraffin wax and mounted in the centre of the bottom of a standard dissolution vessel<sup>27</sup>. Each dissolution experiment was performed in triplicate, as long as the dissolving disc kept a visibly constant surface area.

Intrinsic dissolution studies were performed with a type 2 dissolution test apparatus (VanKel VK7000 dissolution test station) equipped with VK650 heater/circulator<sup>5</sup>. The rotation speed of the paddle was set to 100 rpm. 900 mL of deionized, degassed water was used as the dissolution medium, equilibrated at 37 °C. To sample the dissolution medium a standard dissolution vessel was equipped with a medium recirculation system. The dissolution medium was constantly circulating using a LSMatec peristaltic pump fitted with a  $0.45 \text{ }\mu\text{m}$  filter through a 2 mm flow-through UV cuvette placed in a Cecil CE2020 UV-spectrophotometer set to  $276 \text{ nm}$ <sup>28</sup>. The rate of medium circulation was set to 25 mL/min and the pH of the aqueous medium was monitored using a Thermo Orion 420+ pH-meter.

### **Statistical analysis**

Statistical analysis was carried out using Minitab<sup>TM</sup> statistical software, version 14 (Minitab Inc, USA). Two sample t-tests were carried out at a significance level of 0.05, with a p-value less than 0.05 taken as indicating that the observed difference between the means was statistically significant, i.e. rejecting the null hypothesis.

### **Data analysis**

ACD/Chem Sketch<sup>TM</sup> freeware was used to calculate theoretical element contributions for elemental analysis and partial polarizability volumes<sup>29</sup>.

## Results and discussion

### Single crystal X-ray analysis

Single crystal analysis of SA and salbutamol succinate SSU.MeOH was undertaken, of which details are shown in Table 1. Crystals of SA are centrosymmetric, with both enantiomers present in the lattice. Figure 1a presents the atomic labelling in the unit-cell of the adipate system, which has a 1:1 ratio of salbutamol base to adipic acid. The adipate exists in the lattice in both protonated [O(5)] and ionized [(O(6), O(7))] forms, as shown by the C-O distances: 1.322(2) Å for the protonated form, and C(17)-O(6): 1.265(1) Å and C(17)-O(7): 1.261(2) Å for the ionized form. In addition, there is some disorder in the hydroxyl group on the stereogenic centre, C(8). Further views of the crystal packing are depicted in Figure 2 a, b.

Crystals of SSU.MeOH (Figure 1b) are also centrosymmetric and were determined to be solvated with methanol molecules (Figure 2c and 2d). This was subsequently confirmed by DSC, TGA, elemental analysis and  $^1\text{H}$  NMR spectroscopy. The succinate was found in its ionized form, with C-O bond distances of 1.274(1) Å and 1.253(2) Å. The SSU.MeOH stoichiometry was 2:1:4.

### Analysis of hydrogen bond network

Analysis of the hydrogen bonds in SA (Table 2) reveals that the vast majority of these bonds occur between the hydroxyl groups on the salbutamol and the ionized adipic carboxylate. This carboxylate is also hydrogen bonded to the secondary amine group of salbutamol. The protonated adipic acid does not play a crucial role in the creation of the hydrogen bond network, with only one hydrogen bond to a hydroxyl group of the salbutamol molecule.

Interestingly, analysis of the hydrogen bonds in methanolated salbutamol succinate (Table 3) reveals the crucial role of the methanol in the formation of the lattice and no significant interaction with the ionized succinate. Two molecules of methanol are hydrogen bonded together. There is an O-H...O interaction with the hydroxyl group of salbutamol, as well as O-H...O hydrogen bonding between the methanol

hydroxyl group and salbutamol. In addition, the carboxylate of the succinate interacts with the secondary amine and a hydroxyl group of salbutamol.

A comparison of the crystal packing of SSA (Fig. 2a,b) with SSU.MeOH (Fig. 2c,d) indicates why SSA contains an “additional” protonated molecule of adipic acid. It can be seen that SSA molecules packing along the c axis (Fig. 2b) consists of channels made of salbutamol molecules. These channels are placed centrally around the molecules of adipic acid. The adipic acid molecules are placed one below the other, alternating ionized with protonated molecules in each layer. The ionized carboxylic groups of adipic acid face towards the secondary amine moieties of salbutamol molecules, while protonated groups are placed in close proximity to methoxys of the benzene ring of salbutamol molecules. This indicates that the ionized acid stabilizes more polar parts of the salbutamol molecule, where partial polarizability of R-NH-Me-MeOH molecule fragment was calculated to be  $\alpha$ :  $15.68 \pm 0.5 \text{ \AA}^3$  while the protonated molecule is responsible for interaction with less polar parts of salbutamol, where partial polarizability of HOMe-Ar part was calculated to be:  $\alpha$   $12.96 \pm 0.5 \text{ \AA}^3$ . The interaction is promoted by the close proximity of carboxylic acid groups to the channels formed by salbutamol molecules. This is due to the similar length of adipic acid to the length of the between-salbutamol channel, i.e. approximately 8 Å -O(5)-O(5) distance.

Succinic acid is much shorter than adipic acid, the O(5)-O(4) distance is approximately 5 Å, and forms a different arrangement to SSA along the c axis. Despite the fact that the pKa(s)<sub>1,2</sub> of succinic acid (4.21 and 5.64 at 25 °C)<sup>11</sup> and adipic acid (4.44 and 5.44 at 25 °C)<sup>11</sup> are only slightly different, this difference seems to be large enough to allow ionized succinic acid to stabilize the amine group and neighboring hydroxyl of salbutamol simultaneously. In SSU.MeOH each salbutamol molecule is stabilized, as described, by a succinic acid from the one side and a second molecule of salbutamol, in that the amine group of SB(A) interacts with the hydroxyl next to the amine group of SB(B). The solvated nature of SSU.MeOH arises from the interaction of H-bond dimers (as later described in hydrogen bond network analysis) of methanol with hydroxyls of salbutamol.

Haynes and co-workers presented a review reporting the occurrence of pharmaceutically acceptable anions and cations in the Cambridge Structural Database (CSD)<sup>30</sup>. No examples of a co-crystal of a salt of adipic acid were reported and only 23 co-crystalline forms of adipic acid were found. The same report indicated the occurrence of only 9 salts of succinic acid indicating that both forms of salbutamol presented here are rare in terms of their solid state structures. The SA reported in the current work should be classified as a co-crystal of the salbutamol hemiadipate salt with adipic acid in contrast to the previously reported ethanolated salt of salbutamol hemiadipate<sup>2</sup>.

Previously, a co-crystal of the salt of the API with an unionized counterion was reported for the anticonvulsant drug valproic acid, where the API comprised co-crystalline form of sodium valproate salt with valproic acid<sup>31</sup>. The use of co-crystals in a similar manner to salts in order to alter the physicochemical properties of API has been comprehensively investigated<sup>32-38</sup>, though only one paper published so far reports on the co-existence of dianions and an unionized form of the acid in the same crystal lattice, similarly to what we have determined for SA, it was a hydrated crystal of escitalopram oxalate with oxalic acid<sup>39</sup>.

### **Hirshfeld surfaces analysis**

Hirshfeld surfaces analysis (Fig. 3) allowed for visualization and comparison of reciprocal interactions among atoms in crystal lattices of salbutamol base and salbutamol sulfate compared to salbutamol adipate and succinate. The visualization is based on a 3-D surface surrounding a single molecule of salbutamol.

Noticeably, the same chemical structure of salbutamol may present different intensity of reciprocal interactions externally and internally to the Hirshfeld surface. Red places named “hot spots”, indicate areas of salbutamol molecules where the interactions are the strongest and the distance between attracting atoms is shorter than in the case of attraction caused by Van der Waals forces (corresponding to white colour on Hirshfeld surface). In all of the derivatives of salbutamol, the most involved areas in the formation of hot spots include hydroxyl groups, where hydrogens and oxygens generate separate,



independent crystallographically hot spots and the secondary amine group. Hirshfeld surface analysis also confirmed that hydrogens of methyl groups of the butyl moiety, secondary methyl group and hydrogens of the benzene ring are able to form weak hot spot interactions. It is evident that the molecule of salbutamol in the crystal structure of SB forms an intensive hot spot interactions close to O(1)–H(1), the same as in co-crystalline form of SA, while this interaction is visibly weaker for salbutamol molecules forming crystal structures of salt forms SS and SSU.MeOH. The intensity of hot spot interaction also differs in the case of the methoxyl group O(3)–H(3) attached to the benzene ring of salbutamol. Involvement in the strongest (the most intense red color) interaction was for O(3) of SB, a slightly weaker interaction was demonstrated by H(3) in crystal structures of SA and SSU.MeOH, while O(3) contact lost its intensity. The SS structure presented two weak hot spots, one from the oxygen and the other from hydrogen atom. The weakest intensity and distribution on Hirshfeld surface of hot spot interactions was for salbutamol base and its co-crystalline form. The hot spot interactions identified corresponded well with detected H-bond interactions for SA and SSU listed in tables 3 and 4.

### **Results of PXRD analysis**

The theoretical powder pattern of SA generated from the single crystal X-ray analysis at 100 K (Figure 4 a) is consistent with the powder XRD pattern of the bulk material determined at ambient conditions (Figure 4 b). There are small differences between the two patterns, which most likely can be attributed to thermal anisotropic expansion of the lattice.

The bulk material consisted of colorless, transparent, rhomboidal, thin, plate-like crystals.

Results of PXRD analysis of SSU.MeOH (Fig. 5 b) are also consistent with the theoretical PXRD pattern (Fig. 5 a). Again, small differences between the two patterns can be attributed to the different temperatures used for the experiments. Figure 8 c presents the PXRD pattern of desolvated SSU. Broadening and lower intensity of the Bragg peaks may be indicative of damage to the crystal lattice.

## NMR results

Table 4 compares  $^1\text{H}$  NMR data recorded for SB and the following salts: SS, SA, SSU.MeOH and SSU. Results obtained for SB are consistent with data previously reported by Regla et al. (1997)<sup>40</sup>.  $^1\text{H}$  NMR confirmed the presence of methanol in the crystal structure due to the methyl group (3.18 ppm), which was absent in the desolvated form. Slight shifts in peak positions between SB and salbutamol salt forms may be ascribed to interactions of molecules of dissolved APIs with DMSO. Results of  $^{13}\text{C}$  NMR analysis are listed in Table 5. The number and position of the carbon peaks correlate well with data reported by Regla et al. (1997)<sup>40</sup> for SB. The carbons of adipic acid appeared as three peaks corresponding to 6 symmetrical carbons and the carbons of succinic acid showed as two peaks corresponding to 4 symmetrical carbons. The  $^{13}\text{C}$  NMR also detected the carbons (17,16) of methanol in the solvated form of SSU.MeOH and their absence in the desolvated form (SSU).

## Stoichiometry and elemental analysis

Elemental analysis confirms the molar ratio of salbutamol and adipic acid in SA is 1:1 (Table 6).

Elemental analysis of SSU.MeOH correlates well with single crystal X-ray analysis data suggesting a ratio of two molecules of salbutamol to one molecule of succinic acid to four molecules of methanol, the presence of which in the crystallized material was confirmed by NMR analysis. Results for the solvated material have greater variation due to solvate instability at ambient conditions and methanol evaporation. Results of elemental analysis confirm that the molar ratio of salbutamol to succinic acid in SSU is 2:1.

## Thermal analysis

Thermal analysis (TGA) of SA did not indicate a significant mass loss on drying at the beginning of the scan. Overall mass loss recorded during the TGA scan (Fig. 6 a) up to 100 °C was  $0.94 \pm 0.03\%$  of initial mass of the sample. DSC analysis of the material showed a single strong endothermic event (Fig. 6 d) related to melting with decomposition at  $181.00 \pm 0.04$  °C, correlating with the beginning of significant further mass loss in the TGA. The melting point of adipic was measured to be at  $150.93 \pm 0.10$  °C.

DSC analysis of SSU.MeOH (Fig. 6 e) indicated a large broad endotherm with an onset at  $69.97 \pm 0.30$  °C and enthalpy of 139.43 J/g. These endothermic events correlated well with the sample mass loss due to liberation of methanol (Fig. 6 b) of  $17.26 \pm 1.20\%$ . The theoretical content of solvated methanol was calculated to be 17.68%.

The onset of thermal decomposition after desolvation was recorded to be  $179.23 \pm 0.10$  °C and corresponded with further significant mass loss. In contrast, succinic acid melted at  $185.90 \pm 0.21$  °C. There was a  $0.80 \pm 0.02\%$  overall mass loss up to 100°C in the TGA determined for SSU (Fig. 6 c, f) indicating very slight drying. Onset of thermal decomposition was recorded at  $182.83 \pm 0.15$  °C.

The onsets of thermal decomposition of the new salbutamol forms were consistent with the onset of decomposition of about 180 °C<sup>41</sup> for SS. Thus it can be concluded that the new forms and SS have similar thermal stability.

## FT-IR analysis

The FTIR patterns of SA (Fig. 7 c) and SSU (Fig. 8 d) differ in comparison to spectra of the parent compounds (Fig. 7 a, b, e). The main difference between SSA, SSU and SB is the strong suppression of conjugated C=C stretching vibrations of benzene ring of salbutamol just above  $1600\text{ cm}^{-1}$  and changes in the intensity of the carboxylic acid C=O stretch peaks. The stretching vibration of N-H band of salbutamol (Fig. 7 e) recorded at  $3300\text{ cm}^{-1}$  for SB was nearly completely suppressed and slightly shifted towards longer wavelengths in SSU (Fig. 7 d) indicating a complete ionization of the secondary amine group. In contrast, the N-H stretching vibration of the secondary amine group in SA (Fig. 7 c) is

relatively noticeable with a strong shift to  $3450\text{ cm}^{-1}$ . These observations agree with the single crystal X-ray data suggesting a co-crystal form of SA, where one out of two adipic acid molecules per two molecules of salbutamol base remains unionized, but strongly H-bonded to the secondary amine group of salbutamol. The co-crystal versus salt forms of salbutamol are clearly distinguishable by FTIR, where the broad stretching vibration of C=O of the acid in SSU has been completely suppressed, while the acidic carbonyl group vibration in SA remained highly visible with a slight shift towards longer wavelengths.

### **Dynamic Vapor Sorption (DVS)**

Both SSU and SA do not adsorb more than 2% of moisture and under the conditions of dynamic vapor sorption analysis do not tend to form hydrates (Fig. 8). Results of equilibration of SSU at any given RH%, regardless of whether assessed in the sorption or desorption stage, are similar to SS, and in both cases the amount of adsorbed liquid does not exceed 0.3% of initial sample mass at 90% RH. In the case of SA sample less than 1.6% of initial mass was adsorbed at 90% RH.

Since the moisture sorption behavior may be attributed to the powder surface area, the samples subjected to the DVS analysis were also characterized in terms of their specific surface area and particle size. The specific surface area ( $T_{\text{BET}}$ ) of SS was measured to be  $1.53 \pm 0.02\text{ m}^2/\text{g}$ , that of SA was  $1.81 \pm 0.02\text{ m}^2/\text{g}$  and  $T_{\text{BET}}$  of SSU was  $2.26 \pm 0.06\text{ m}^2/\text{g}$ . The median particle size determined was  $8.09 \pm 0.18$ ,  $19.26 \pm 0.07$  and  $8.73 \pm 0.09\text{ }\mu\text{m}$  for SS, SA and SSU, respectively. It is possible, therefore, that the higher propensity of SA to sorb moisture may be due to the different particle size, but cannot be explained by the difference in the surface area. It is likely that other surface properties, such as surface energy, contribute to this effect and will be the subject of further studies.

## Solubility and dissolution studies

The estimated aqueous solubilities of SA, SSU and SB were found to be  $82 \pm 2$  mg/ml (equivalent to  $0.231 \pm 0.001$  M of salbutamol) at pH  $4.5 \pm 0.1$ ,  $334 \pm 13$  mg/ml (equivalent to  $1.183 \pm 0.045$  M of salbutamol) at pH  $6.6 \pm 0.1$  and  $2.63 \pm 0.09$  mg/ml (equivalent to  $0.0110 \pm 0.0004$  M of salbutamol) at pH  $10.0 \pm 0.1$ , respectively. Thus the improvement in solubility, compared to SB, was 21- and 108-fold for the drug presented as SA and SSU, respectively, indicating that SSU has a 5-fold greater solubility than SA.

As the new forms of salbutamol are composed of the drug and co-former that are able to ionize in solution, it is expected that the pH of the saturated medium may have a profound effect on the solubility of the compounds<sup>11</sup>. This was investigated for SA, as it was easier to change the pH for this compound due to the lower solubility in comparison to SSU. When the pH of medium was adjusted to 5.3, the solubility of SA was measured to be  $60 \pm 1$  mg/ml.

Equations describing the solubility of gabapentin/3-hydroxybenzoic acid cocrystal,<sup>42</sup> and carbamazepine and itraconazole cocrystals have been reported<sup>43</sup>. These models allow relationships between the pH and co-crystal solubility to be predicted knowing only the solubility product constant ( $K_{sp}$ ) and acid dissociation constants of the cocrystal constituents ( $pK_a$ s). Although the theoretically-derived models neglect nonidealities due to complexation and other specific interactions, very good agreements between the calculated and experimental values were observed<sup>42,43</sup>. This approach was employed in this work as the authors suggest that cocrystal solubility and its pH relationship may be estimated from a single measurement<sup>43</sup>. Similar mathematical equations were therefore developed for the new salbutamol forms to predict their solubility-pH dependence and estimate the solubility difference in relation to the pure drug. The co-formers and the drug have acidic and amphoteric characteristics, respectively, therefore the previously reported equations were adapted, taking into consideration that each of the species has two  $pK_a$  values and that the stoichiometry of the succinate form is 2:1.

SA has a molar ratio 1:1, hence the equation for equilibrium reaction describing dissociation of the cocrystal in solution is as follows:

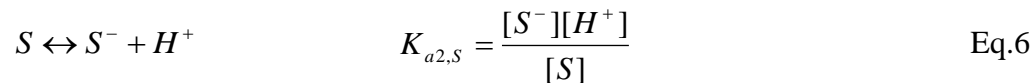
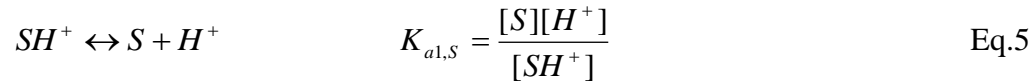
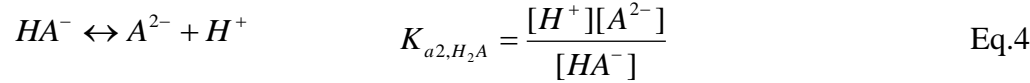
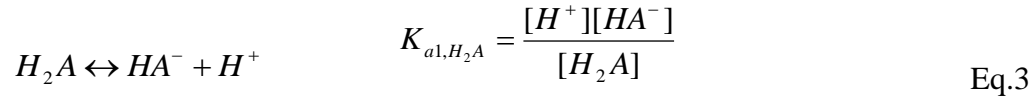


where S-H<sub>2</sub>A is the cocrystal/salt in the solid phase, S<sub>solution</sub> and H<sub>2</sub>A<sub>solution</sub> are equilibrium solubilities of the drug and acid, respectively, thus

$$K_{sp} = \frac{[S][H_2A]}{[S - H_2A]}, \text{ and with S-H}_2\text{A in the solid phase the } K_{sp} \text{ can be presented as:}$$

$$K_{sp} = [S][H_2A] \Rightarrow [H_2A] = \frac{K_{sp}}{[S]} \quad \text{Eq.2}$$

Equilibrium reactions for adipic acid and salbutamol are presented in Eqs. 3 and 4 (for the acid) and Eqs. 5 and 6 (for the drug).



where [HA<sup>-</sup>], [A<sup>2-</sup>] are concentrations of the monodissociated and fully dissociated acid species and [SH<sup>+</sup>], [S] are concentrations of protonated and monobasic salbutamol species.

Combining the total acid and drug concentrations, the solubility of salbutamol adipate can be expressed as (Eq.7):

$$S_{\text{cocrystal}} = \sqrt{K_{sp} \cdot \left(1 + \frac{K_{a1,H_2A}}{[H^+]} + \frac{K_{a2,H_2A} \cdot K_{a1,H_2A}}{[H^+]^2}\right) \cdot \left(1 + \frac{[H^+]}{K_{a1,S}} + \frac{K_{a2,S}}{[H^+]}\right)} \quad \text{Eq. 7}$$

where  $S_{\text{cocystal}}$  is cocystal solubility,  $K_{a1,H_2A}$  and  $K_{a2,H_2A}$  are the first and second dissociation constants for the acid and  $K_{a1,S}$  and  $K_{a2,S}$  are the first and second dissociation constants for the drug.

Using a similar approach, the equation for salbutamol succinate, considering the 2:1 stoichiometry, is as follows (Eq. 8):

$$S_{\text{salt}} = \sqrt[3]{\frac{K_{sp}}{4} \left(1 + \frac{K_{a1,H_2A}}{[H^+]} + \frac{K_{a2,H_2A} \cdot K_{a1,H_2A}}{[H^+]^2}\right) \cdot \left(1 + \frac{[H^+]}{K_{a1,S}} + \frac{K_{a2,S}}{[H^+]}\right)^2} \quad \text{Eq. 8}$$

The  $pK_{sp}$  constants for salbutamol adipate and succinate, calculated using the aqueous solubility values, were 6.3 and 8.6, respectively. Substituting in  $pK_a$  values as follows:  $pK_{a1}=4.44$ ,  $pK_{a2}=5.44$  for adipic acid<sup>11</sup>,  $pK_{a1}=4.21$ ,  $pK_{a2}=5.64$  for succinic acid<sup>11</sup> and  $pK_{a1}=9.1$ ,  $pK_{a2}=10.4$  for salbutamol<sup>17</sup>, the pH-solubility profiles derived from Eqs. 8 and 9 are presented in Fig. 9. The theoretical models suggest that a minimum SA solubility occurs at pH around 5 and that of SSU at pH 7.

The comparison of intrinsic dissolution rates (IDRs) of salbutamol from SA (4.18 mg/cm<sup>2</sup>/min,  $R^2$  of 0.999) and SSU (14.94 mg/cm<sup>2</sup>/min,  $R^2$  of 0.997) with that of salbutamol sulfate (15.47 mg/cm<sup>2</sup>/min,  $R^2$  of 0.999) (Fig. 10) reveals that the rate of salbutamol release from SA is lower than that from SS or SSU. The IDR of salbutamol from SA is ~4 times lower and significantly different ( $p<0.05$ ) than that of the other salt forms, consistent with the ~5-fold difference in salbutamol solubility. There was no significant difference ( $p=0.865$ ) between the IDRs of salbutamol in SS and SSU. Our results for the co-crystal of the salbutamol hemiadipate salt with adipic acid (SA) contrasts with that of Jashnani et al.<sup>2</sup> who obtained a salbutamol hemiadipate diethanolate which had an IDR equivalent to SS.

Interestingly, the difference in the IDR values obtained reflect the different acid solubilities i.e. the saturated solubility of succinic acid at 20 °C is reported to be 7.7% w/v and that of adipic acid to be 1.8% w/v<sup>45</sup>, therefore it may be expected that the solubility of salbutamol adipate is lower than that of salbutamol succinate.

## Conclusions

Despite the chemical similarity of succinic and adipic acids, the solid state properties of their salbutamol salts when made by the same methods are significantly different. For the first time we reported the involvement of adipic acid molecule in the formation of a co-crystal of a salt. Salbutamol succinate is a rare example of the succinate constituting a solvated salt form with API molecule. The intrinsic dissolution rate of salbutamol in SSU was around 4-fold greater than that of SA, consistent with the ~5-fold difference in aqueous solubility of salbutamol in SA and SSU, thus the difference in the intrinsic dissolution rates was comparable to the solubility trend. Both materials presented similar thermal stability and did not undergo hydration under increasing humidity. The effectiveness of anion choice as a modification of *in vivo* bioavailability of salbutamol needs further investigations, as the concept of retarding dissolution of an API by the formation of an appropriate salt/co-crystal is a promising approach, which may alleviate some issues associated with formulation of extended release dosage forms such as component compatibility and regulatory approval for the use of excipients.

Results described here show that salt and/or co-crystal formation remains largely unpredictable and requires predominantly empirical screening. The arrangement of molecules in the crystal lattice is dependent on the geometry of the molecules involved and their potential for forming chemical interactions. Even the careful choice of similar counter ions can have a profound effect on the observed crystalline lattice and further work in this area is required.



## **Acknowledgements**

The authors wish to acknowledge funding for this research from the Irish Research Council for Science and Engineering Technology (IRCSET) and the Solid State Pharmaceutical Cluster (SSPC), supported by Science Foundation Ireland under grant number [07/SRC/B1158].

Authors would like to thank Mrs. Ann Connolly University College Dublin, Department of Chemistry, for elemental analysis.

## References

1. BMJ Publishing, British National Formulary: current edition. [electronic resource] accessed 29/10/2010.
2. Jashnani RN, Byron PR, Dalby RN 1993. Preparation, characterization, and dissolution kinetics of two novel albuterol salts. *J Pharm Sci* 82(6): 613- 616.
3. Beale JP, Grainger CT 1972. DL-N-t-Butyl-2(4-hydroxy-3-hydroxymethylphenyl)2-hydroxyethylamine, (salbutamol, Ah. 3365), C<sub>13</sub>H<sub>21</sub>NO<sub>3</sub>. *Cryst Struct Comm* 67(1): 71-74.
4. Leger Par JM, Goursolle M, Gadret EM 1978. Structure Cristalline du Sulfate de Salbutamol [tert-Butylamino-2 (Hydroxy-4 hydroxymethyl-3 phenyl)- 1 Ethanol. ½ H<sub>2</sub>SO<sub>4</sub>]. *Acta Cryst B*34: 1203-1208.
5. Council of Europe 2007. European Pharmacopoeia. 6th ed. 5.4., Strasbourg: Council of Europe.
6. Vyse T, Cochrane GM 1989. Controlled release salbutamol tablets versus sustained release theophylline tablets in the control of reversible obstructive airways disease. *J Int Med Res* 17(1): 93-8.
7. Murthy SN, Shobharani HR 2004. Clinical pharmacokinetic and pharmacodynamic evaluation of transdermal drug delivery systems of salbutamol sulfate. *Int J Pharm* 287: 47–53.
8. Micromedex® Healthcare Series [intranet database]. Version 5.1. Greenwood Village, Colo: Thomson Reuters (Healthcare) Inc.
9. British Pharmacopoeia 2010. ISBN 9780113228287.
10. O'Connor KM, Corrigan OI 2001. Preparation and characterisation of a range of diclofenac Salts. *Int J Pharm* 226: 163–179.
11. Stahl PH, Wermuth CG 2008. Handbook of Pharmaceutical Salts Properties, Selection and use, ISBN 3-906390-26-8.
12. Anderson BD, Conradi RA 1985. Predictive relationships in the water solubility of salts of a nonsteroidal anti-inflammatory drug. *J Pharm Sci* 74(8): 815–820.
13. Veber DF, Johnson SR, Cheng HY, Smith BR, Ward KW, Kopple KD 2002. Molecular properties that influence the oral bioavailability of drug candidates. *J Med Chem* 45: 2615-2623.

14. Li ZJ, Abramov Y, Bordner J, Leonard J, Medek A, Trask AV 2006. Solid-State Acid-Base Interactions in Complexes of Heterocyclic Bases with Dicarboxylic Acids: Crystallography, Hydrogen Bond Analysis, and  $^{15}\text{N}$  NMR Spectroscopy *J Am Chem Soc* 128: 8199-8210.
15. Imboden R, Imanidis G 1999. Effect of the amphoteric properties of salbutamol on its release rate through a propylene control membrane, *Eur J PharmBiopharm* 47: 161-167.
16. FDA, Database of Select Committee on GRAS Substances (SCOGS) Reviews, Succinic acid, <http://www.accessdata.fda.gov/scripts/fcn/fcnDetailNavigation.cfm?rpt=scogsListing&id=339>, accessed 29/10/2010.
17. FDA, Database of Select Committee on GRAS Substances (SCOGS) Reviews, Adipic acid, <http://www.accessdata.fda.gov/scripts/fcn/fcnDetailNavigation.cfm?rpt=scogsListing&id=9>, accessed 29/10/2010.
18. Sheldrick GM 2008. A short history of SHELX. *Acta Cryst A* 64: 112-122.
19. Macrae CF, Bruno I J, Chisholm JA, Edgington PR, McCabe P, Pidcock E, Rodriguez-Monge L, Taylor R, van de Streek J, Wood P A 2008. *J Appl Cryst* 41: 466-470.
20. Tajber L, Corrigan DO, Corrigan OI, Healy AM 2009. Spray drying of budesonide, formoterol fumarate and their composites. I. Physicochemical characterisation. *Int J Pharm* 367: 79-85.
21. Tajber L, Corrigan OI, Healy AM 2005. Physicochemical evaluation of PVP-thiazide diuretic interactions in co-spray-dried composites - analysis of glass transition composition relationships. *Eur J Pharm Sci* 24: 553-563.
22. Healy AM, McDonald BF, Tajber L, Corrigan OI 2008. Characterisation of excipient-free nanoporous microparticles (NPMPs) of bendroflumethiazide. *Eur J Pharm Biopharm* 69: 1182-1186.
23. Paluch KJ, Tajber L, McCabe T, O'Brien JE, Corrigan OI, Healy AM 2010. Preparation and solid state characterisation of chlorothiazide sodium intermolecular self assembly suprastructure, *Eur J Pharm Sci* 41: 603-611.

24. Fadda HM, Sousa T, Carlsson AS, Abrahamsson B, Williams JG, Kumar D, Basit AW 2010. Drug Solubility in Luminal Fluids from Different Regions of the Small and Large Intestine of Humans. *Mol Pharm* 7(5): 1527–1532.
25. Thoma K, Ziegler I 1998. Simultaneous quantification of released succinic acid and a weakly basic drug compound in dissolution media. *Eur J Pharm Biopharm* 46: 183–190.
26. Kordis-Krapez M, Abram V, Kac M, Ferjancic S 2001. Determination of Organic Acids in White Wines by RP-HPLC. *Food Technol Biotechnol* 39: 93-99.
27. Healy AM, Corrigan OI 1996. The influence of excipient particle size, solubility and acid strength on the dissolution of an acidic drug from two-component compacts. *Int J Pharm* 143(2): 211-221.
28. Nocent M, Bertocchi L, Espitalier F, Baron M, Couarraze G 2001. Definition of a Solvent System for Spherical Crystallization of Salbutamol Sulfate by Quasi-Emulsion Solvent Diffusion (QESD) Method. *J Pharm Sci* 90(10): 1620-7.
29. Gad E, Mahmoud A, Khairou KS 2008. QSPR for HLB of Nonionic Surfactants Based on Polyoxyethylene Group. *J Disper Sci Technol* 29(7): 940 – 947.
30. Haynes DA, Jones W, Motherwell WDS 2005. Occurrence of pharmaceutically acceptable anions and cations in the Cambridge structural database. *J Pharm Sci* 94: 2111-2120.
31. Petrusevski G, Naumov P, Jovanovski G, Bogoeva-Gaceva G, Weng Ng S 2008. Solid-State Forms of Sodium Valproate, Active Component of the Anticonvulsant Drug Epilim *Chem Med Chem* 3: 1377 – 1386.
32. Bailey RD, Walsh MW, Bradner S, Fleischman L, Morales A, Moulton B, Rodríguez-Hornedo N, Zaworotko MJ 2003. Crystal engineering of the composition of pharmaceutical phases, *Chem Commun* 2003: 186–187.
33. McNamara DP, Childs SL, Giordano J, Iarriccio A, Cassidy J, Shet MS, Mannion R, O'Donnell E, Park A 2006. Use of a Glutaric Acid Cocrystal to Improve Oral Bioavailability of a Low Solubility API *Pharm Res* 23(8): 1888-1897.

34. Variankaval N, Wenslow R, Murry J, Hartman R, Helmy R, Kwong E, Clas SD, Dalton C, Santos I 2006. Preparation and solid-state characterization of nonstoichiometric cocrystals of a phosphodiesterase- IV inhibitor and l-tartaric acid. *Cryst Growth Des* 6: 690–700.
35. Zegarac M 2007. Pharmaceutically acceptable co crystalline forms of sildenafil. WO080362 A1. 2007.
36. Shan N, Zaworotko MJ 2008. The role of cocrystals in pharmaceutical Science, *Drug Discov Today* 13 (9-10) 440-446.
37. Dova E, Mazurek JM, Anker J 2008. Tenofovir Disoproxil Hemi-Fumaric Acid Co-Crystal WO/2008/143500.
38. Cheney ML, Shan N, Healey ER, Mazen H, Wojtas Ł, Zaworotko MJ, Sava V, Song S, Sanchez-Ramos JR 2010. Effects of Crystal Form on Solubility and Pharmacokinetics: A Crystal Engineering Case Study of Lamotrigine. *Cryst Growth Des* 10(1): 394–405.
39. Harrison WTA, Yathirajan HS, Bindya S, Anilkumar HG, Devaraju 2007. Escitalopram oxalate: co-existence of oxalate dianions and oxalic acid molecules in the same crystal. *Acta Cryst C* 63: 129-131.
40. Regla I, Reyes A, Körber C, Demare P, Estrada O, Juaristi E 1997. Novel Applications of Raney Nickel/Isopropanol: Efficient System for the Reduction of Organic Compounds. *Synthetic Commun* 27(5): 817-823.
41. Larhrib H, Martin GP, Marriott C, Prime D 2003. The influence of carrier and drug morphology on drug delivery from dry powder formulations. *Int J Pharm* 257: 283–296.
42. Sreenivas RL, Bethune S J, Kampf JW, Rodriguez Hornedo N 2009. Cocrystals and Salts of Gabapentin: pH Dependent Cocrystal Stability and Solubility. *Cryst Growth Des* 9(1): 378-385.
43. Bethune SJ, Huang N, Jayasankar A, Rodriguez-Hornedo N 2009. Understanding and Predicting the Effect of Cocrystal Components and pH on Cocrystal Solubility. *Cryst Growth Des* 9(9): 3976–3988.
44. Yazan Y, Demirel M, Güler E 1995. Preparation and in vitro dissolution of salbutamol sulfate microcapsules and tableted microcapsules. *Journal of Microencapsul* 12: 601-607.

Table 1. Crystallographic data for SA and SSU.MeOH.

|  | SA   | SSU.MeOH   |
|--|--|--|
| Crystal system                                     | triclinic  | monoclinic   |
| Space group, Z                                     | $P\bar{1}$ , 2   | $P 2_1/n$ , 4  |
| Unit cell dimensions,<br>$^\circ$ and $\text{\AA}$ | $a = 9.733(3)$ $\alpha = 66.354(5)$<br>$b = 10.700(3)$ $\beta = 86.080(6)$<br>$c = 10.926(3)$ $\gamma = 67.906(5)$ | $a = 10.3934(5)$<br>$b = 20.2011(10)$ $\beta = 114.5300(10)$<br>$c = 10.3962(5)$ |
| Volume, $\text{\AA}^3$                             | 961.2(4)   | 1985.76(17)  |
| R1 [ $I > 2\sigma(I)$ ], wR2 (all data)            | 0.038, 0.090   | 0.039, 0.104   |

Table 2. Hydrogen bonding in SA.

| D-H...A                       | D-H, $\text{\AA}$ | H...A, $\text{\AA}$ | D...A, $\text{\AA}$ | D-H...A, $^\circ$ |
|-------------------------------|-------------------|---------------------|---------------------|-------------------|
| N1-H1A...O7                   | 0.951(19)         | 1.845(19)           | 2.7945(18)          | 175.6(14)         |
| N1-H1B...O1B                  | 0.96(2)           | 2.404(18)           | 2.808(5)            | 105.0(12)         |
| N1-H1B...O6 <sup>(a)</sup>    | 0.96(2)           | 1.88(2)             | 2.8353(18)          | 172.2(16)         |
| O1A-H1C...O7 <sup>(a)</sup>   | 0.84              | 1.93                | 2.7619(19)          | 169               |
| O1B-H1D...O6 <sup>(a)</sup>   | 0.84              | 2.46                | 2.816(5)            | 106               |
| O1B-H1D...O7 <sup>(a)</sup>   | 0.84              | 1.79                | 2.609(5)            | 166               |
| O2-H2A...O6 <sup>(b)</sup>    | 0.84              | 1.81                | 2.6327(17)          | 165               |
| O3-H3A...O4 <sup>(a)</sup>    | 0.84              | 1.92                | 2.7437(18)          | 167               |
| O5-H5...O3 <sup>(d)</sup>     | 0.88(3)           | 1.76(3)             | 2.6314(18)          | 172(2)            |
| C6-H6...O3                    | 0.95              | 2.50                | 2.8470(19)          | 101               |
| C8-H8B...O2 <sup>(c)</sup>    | 0.99              | 2.54                | 3.457(2)            | 154               |
| C16-H16A...O1B <sup>(a)</sup> | 0.99              | 2.29                | 3.148(5)            | 144               |

Symmetry codes: (a) 1-x, -y, 1-z; (b) 1-x, -y, 2-z; (c) -x, -y, 2-z; (d) 1+x, 1+y, -1+z;

Table 3. Hydrogen bonding in SSU.MeOH.

| <b>D-H...A</b>               | <b>D-H, Å</b> | <b>H...A, Å</b> | <b>D...A, Å</b> | <b>D-H...A, °</b> |
|------------------------------|---------------|-----------------|-----------------|-------------------|
| O1-H1...O5 <sup>(b)</sup>    | 0.84          | 1.79            | 2.6297(14)      | 173               |
| N1-H1A...O4 <sup>(b)</sup>   | 0.929(18)     | 1.852(19)       | 2.7786(15)      | 175.0(13)         |
| N1-H1B...O1 <sup>(c)</sup>   | 0.912(16)     | 1.924(17)       | 2.7953(13)      | 159.1(17)         |
| O2-H2A...O7 <sup>(d)</sup>   | 0.84          | 1.80            | 2.6312(16)      | 171               |
| O3-H3A...O4 <sup>(e)</sup>   | 0.84          | 1.85            | 2.6721(13)      | 165               |
| O6-H6A...O3 <sup>(g)</sup>   | 0.84          | 1.84            | 2.6754(13)      | 174               |
| O7-H29...O6 <sup>(h)</sup>   | 0.84          | 1.81            | 2.6523(15)      | 176               |
| C2-H2...O5 <sup>(a)</sup>    | 0.95          | 2.53            | 3.4744(14)      | 177               |
| C6-H6...O3                   | 0.95          | 2.56            | 2.8788(14)      | 100               |
| C8-H8A...O2 <sup>(e)</sup>   | 0.99          | 2.38            | 3.3068(15)      | 155               |
| C11-H11B...O2 <sup>(f)</sup> | 0.98          | 2.57            | 3.5145(15)      | 162               |

Symmetry codes: (a) 1-x, 2-y, 2-z; (b) 1+x, y, z; (c) 2-x, 2-y, 2-z; (d) x, 1+y, z; (e) 1-x, 2-y, 1-z; (f) 3/2-x, -1/2+y, 3/2-z; (g) x, -1+y, z; (h) -1/2+x, 1/2-y, 1/2+z

Table 4. <sup>1</sup>H NMR analysis of SB and SS, SA, SSU.MeOH and SSU.

| Peak   | SB             |          | SB<br>(Regla at al.<br>1997) <sup>40</sup> | SS             | SA             | SSU.MeOH    | SSU            |
|--|----------------|----------|--|----------------|----------------|-------------|----------------|
|  | v(F1)<br>[ppm] | Integral | v(F1) [ppm]                                | v(F1)<br>[ppm] | v(F1)<br>[ppm] | v(F1) [ppm] | v(F1)<br>[ppm] |
| C(10,11,12)<br>H(10,11,12)                   | 1.02           | 9.08     | 1.02                                       | 1.22           | 1.21           | 1.16        | 1.16           |
| C(8)H(8AB)                                   | 2.54           | 2.79     | 2.55                                       | 2.78           | 2.84           | 2.74        | 2.71           |
| C(7)H(7)                                     | 4.40           | 1.09     | 4.42                                       | 4.69           | 4.70           | 4.61        | 4.59           |
| C(13)H(13AB)                                 | 4.48           | 1.99     | 4.47                                       | 4.50           | 4.48           | 4.59        | 4.49           |
| C(2)H(2)                                     | 6.69           | 1.00     | 6.69                                       | 6.75           | 6.74           | 6.755       | 6.75           |
| C(3)H(3)                                     | 6.99           | 1.02     | 6.99                                       | 7.08           | 7.07           | 7.04        | 7.04           |
| C(6)H(6)                                     | 7.27           | 1.04     | 7.27                                       | 7.34           | 7.32           | 7.31        | 7.31           |
| C(15,18)<br>H(15,18/AB)<br>C(15)<br>H(15/AB) | -              | -        | -  | -              | 2.11           | 2.28        | 2.28           |
| C(16,19)                                     | -              | -        | -  | -              | 1.49           | -           | -              |
| C(16)<br>H(16/ABC)<br>C(17)<br>H(29-31)      | -              | -        | -  | -              | -              | 3.18        | -              |

Table 5. <sup>13</sup>C NMR analysis of SB and SS, SA, SSU.MeOH and SSU.

| Peak                        | SB          | SB (Regla<br>at al.<br>1997) <sup>40</sup> | SS          | SA          | SSU.MeOH    | SSU         |
|-----------------------------|-------------|--|-------------|-------------|-------------|-------------|
|                             | v(F1) [ppm] | v(F1) [ppm]                                | v(F1) [ppm] | v(F1) [ppm] | v(F1) [ppm] | v(F1) [ppm] |
| C(10,11,12)<br>H(10-12/ABC) | 28.9        | 28.74                                      | 26.7        | 26.4        | 27.4        | 27.4        |
| C(9)                        | 49.6        | 49.8                                       | 49.7        | 49.1        | 50.1        | 50.2        |
| C(8)H(8AB)                  | 50.8        | 50.7                                       | 49.6        | 49.6        | 49.98       | 50.0        |
| C(13)H(13AB)                | 58.3        | 58.3                                       | 58.7        | 58.8        | 58.73       | 58.8        |
| C(7)H(7)                    | 72.4        | 72.3                                       | 70.3        | 69.9        | 71.11       | 71.1        |
| C(2)H(2)                    | 114.0       | 114.0                                      | 114.6       | 114.7       | 114.60      | 114.6       |
| C(3)H(3)                    | 124.8       | 124.9                                      | 125.5       | 125.3       | 125.40      | 125.4       |
| C(6)H(6)                    | 125.0       | 125.1                                      | 125.6       | 125.5       | 125.54      | 125.5       |
| C(1,4,5)                    | 127.9       | 127.9                                      | 128.6       | 128.6       | 128.61      | 128.6       |
| C(1,4,5)                    | 134.6       | 134.5                                      | 133.4       | 133.3       | 133.79      | 133.8       |
| C(1,4,5)                    | 153.1       | 153.1                                      | 153.9       | 154.0       | 153.90      | 153.9       |
| C(14,17)                    | -           | -  | -           | 176.7       | 176.18      | 176.2       |
| C(15,18)                    | -           | -  | -           | 35.9        | 32.92       | 32.9        |
| C(16,19)                    | -           | -  | -           | 25.6        | -           | -           |
| C(17,16)                    | -           | -  | -           | -           | 49.06       | -           |



Table 6. Comparison of theoretical values and experimental results of elemental analysis of carbon, nitrogen and hydrogen contents in salbutamol salts.

| Content (% w/w) |              | C %         | H %       | N %       |
|-----------------|--------------|-------------|-----------|-----------|
| SA              | Theory 1:1   | 59.20       | 8.11      | 3.63      |
|                 | Experimental | 59.00±0.01  | 8.20±0.08 | 3.68±0.07 |
| SSU.MeOH        | Theory       | 56.34       | 8.90      | 3.86      |
|                 | Experimental | 56.53±0.37  | 8.19±0.18 | 3.59±0.53 |
| SSU             | Theory 2:1   | 60.38       | 8.11      | 4.69      |
|                 | Experimental | 60.275±0.05 | 8.01±0.07 | 4.61±0.01 |

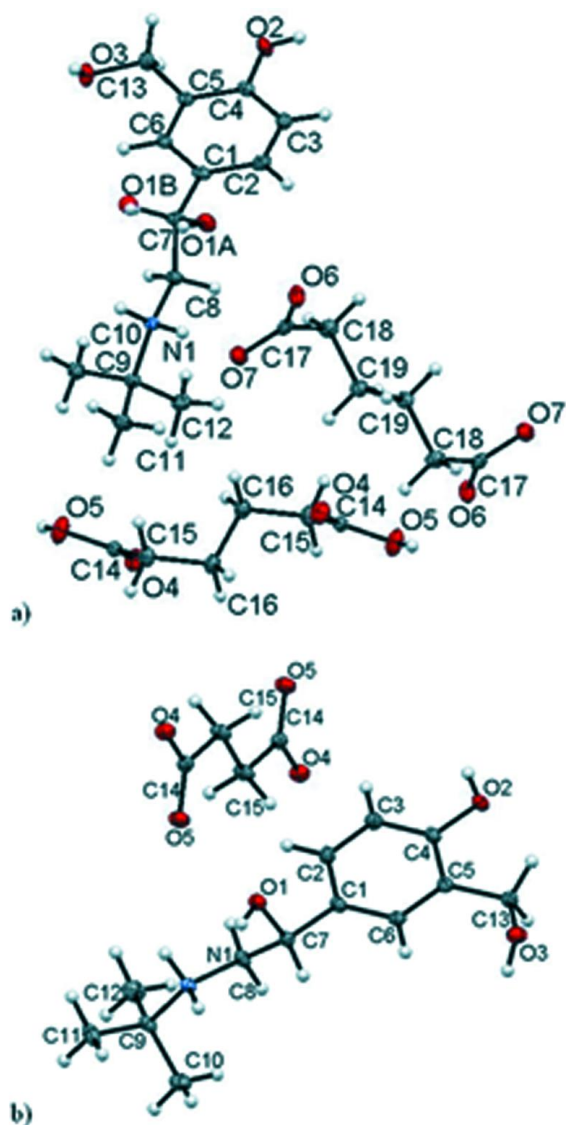


Fig. 1. a) SA and b) SSU.MeOH showing the atomic labelling. The solvent molecules in SSU.MeOH are omitted for clarity. Probability ellipsoids are shown at the 50% level.

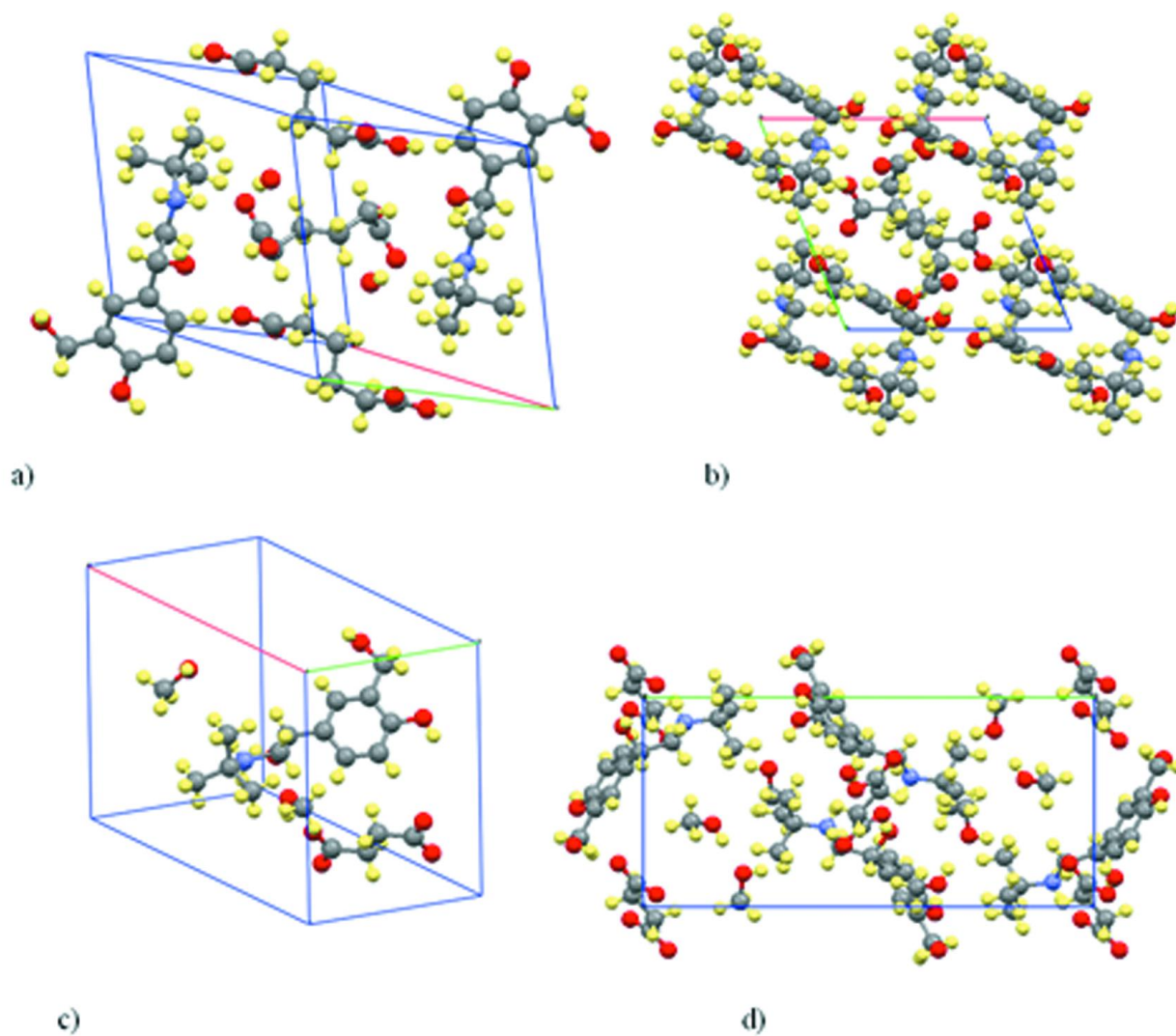


Fig. 2. a) unit cell of SA, b) extended packing diagram of SA along c axis, c) unit cell of SSU.MeOH, d) extended packing diagram of SSU.MeOH along b axis.

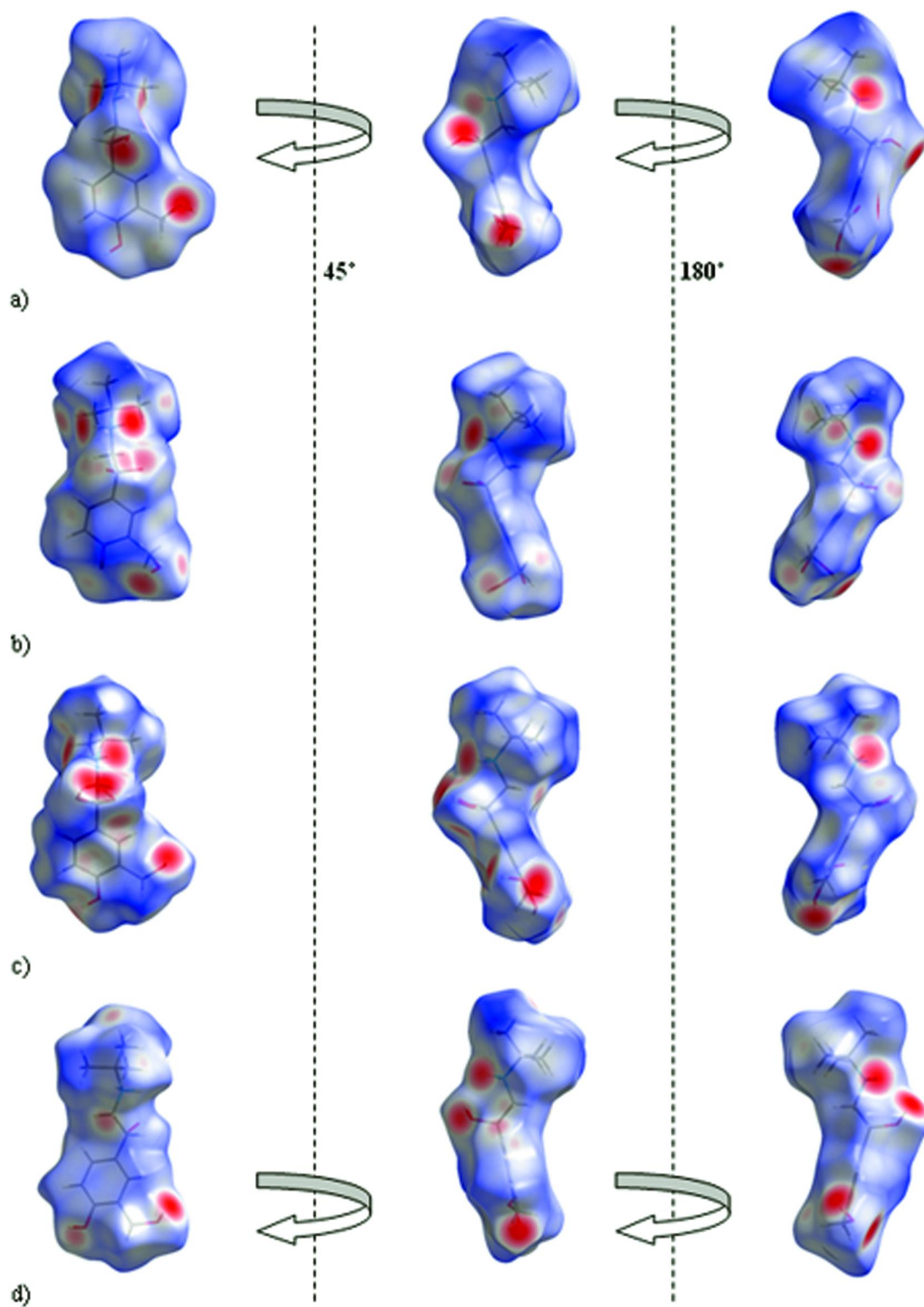


Fig. 3. Hirschfield surfaces of: a) SB, b) SS, c) SA and d) SSU.

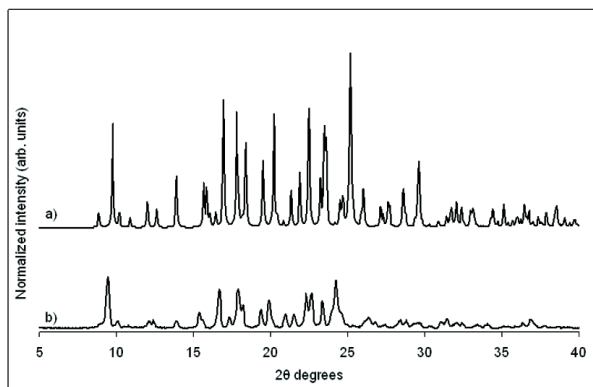


Fig. 4. Comparison of SA PXRD patterns: a) theoretical pattern, b) experimental diffractogram.

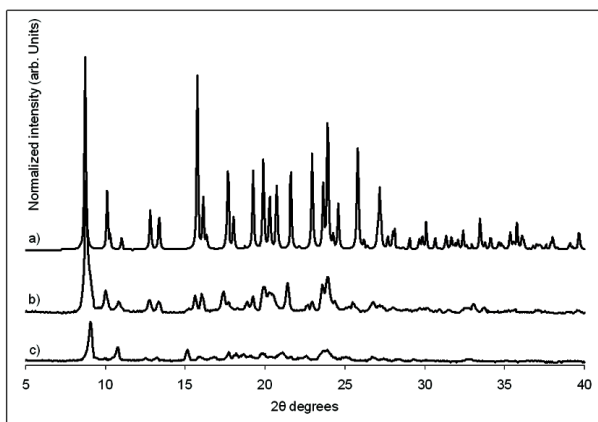


Fig. 5. Comparison of PXRD patterns: a) SSU.MeOH theoretical pattern, b) SSU.MeOH experimental diffractogram and c) SSU experimental diffractogram.

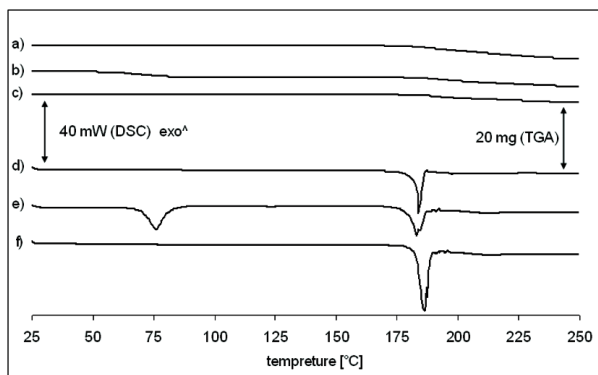


Fig. 6. Thermal analysis: a) TGA scan of SA, b) TGA scan of SSU.MeOH, c) TGA scan of SSU, d) DSC of SA, e) DSC scan of SSU.MeOH, f) DSC scan of SSU.

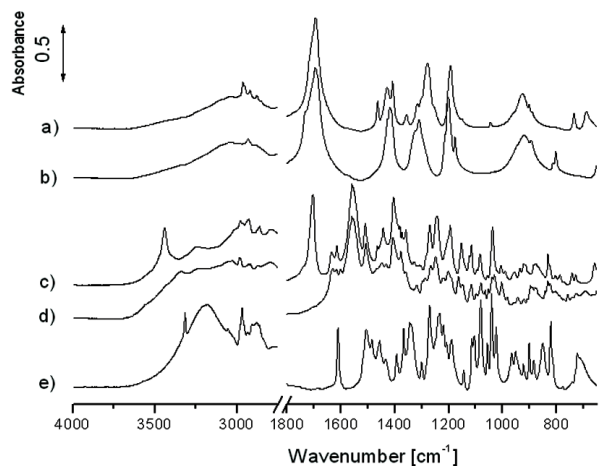


Fig. 7. FTIR spectra of: a) adipic acid, b) succinic acid, c) SA, d) SSU, e) SB.

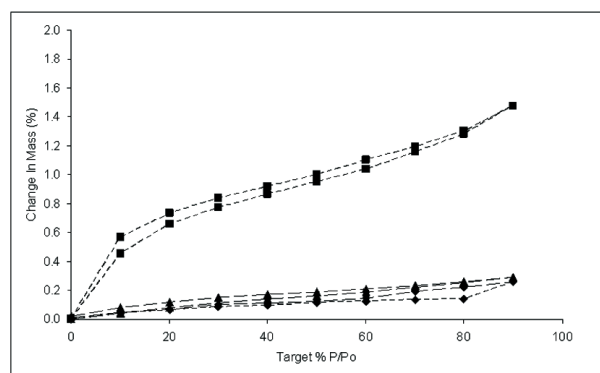


Fig. 8. Dynamic Vapor Sorption of: SA (squares), b) SSU (triangles), c) SB (diamonds).

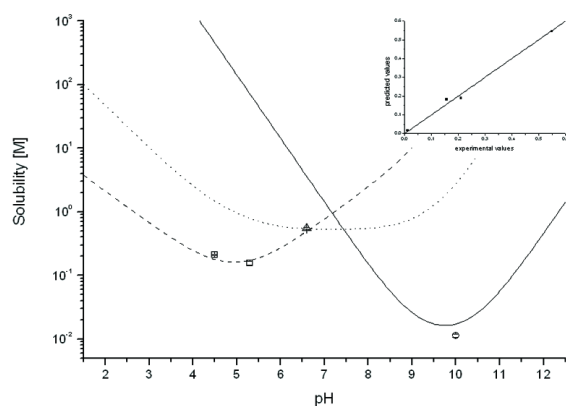


Fig. 9. Theoretical profiles describing pH-solubility dependence for SA (dashed line), SSU (dotted line) and SB (solid line). Empty squares indicate experimental solubility values for SA, the triangle for SSU and the circle shows the experimental solubility of SB. The inset shows a correlation ( $y=x$ ) between the experimental and predicted data points.

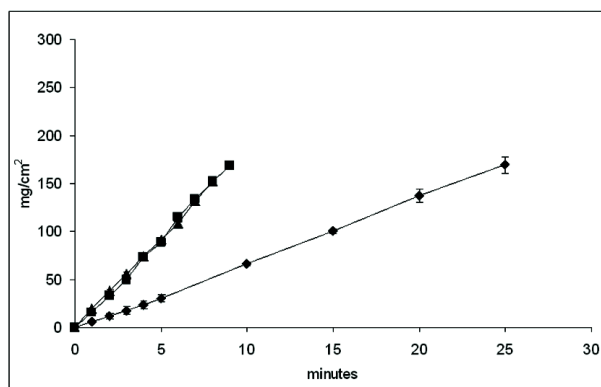


Fig. 10. Intrinsic dissolution profiles of SA (diamonds) and SSU (squares) and SS (triangles).